Light-Actuated Digital Microfluidics for Large-Scale Droplet Manipulation

Shao Ning Pei
Ming C. Wu

Electrical Engineering and Computer Sciences
University of California at Berkeley

Technical Report No. UCB/EECS-2011-124
http://www.eecs.berkeley.edu/Pubs/TechRpts/2011/EECS-2011-124.html

December 6, 2011

Light-Actuated Digital Microfluidics for Large-Scale Droplet Manipulation

by Shao Ning Pei

Research Project Report

Submitted to the Department of Electrical Engineering and Computer Sciences, University of California at Berkeley, in partial satisfaction of the requirements for the degree of **Master of Science, Plan II**.

Approval for the Report:

Professor Ming C. Wu

Research Advisor

(Date)

* * * * * * *

Professor Michel Maharbiz

Second Reader

(Date)

Abstract

The ability to quickly perform a large number of chemical or biological reactions in parallel using low reagent volumes is a field well addressed by electrowetting-based digital microfluidics. Here we report on a new light-actuated digital microfluidics device which uses on-demand, 'virtual' electrodes defined by light patterns from a data projector for the large-scale, parallel manipulation of arbitrarily sized droplets. The device features a thin, high-quality aluminum oxide film deposited via atomic layer deposition (ALD), which allows aggressive scaling of the dielectric thickness while maintaining high device reliability. Due to the thin ALD dielectric layer, a significantly higher actuation force is imparted on droplets, which results in actuation speeds of up to 2 cm/s. Compared to our previous device, the actuation speed is 20x faster, but achieved at 250x lower optical power and 5x lower voltage. In this paper, we demonstrate the device's ability to perform all the critical digital microfluidics functionalities: transport, creation, merging, and splitting. In addition, the ability to easily achieve parallel manipulation and array formation (8 by 12, 96 droplet format) of droplets will be presented.

Introduction

Electrowetting-on-dielectric (EWOD) based digital microfluidics[1,2] is a microscale liquid-handling technique where discrete liquid droplets are manipulated over a two-dimensional surface. Compared to continuous channel-flow based microfluidic techniques, digital microfluidics eliminates the need for bulky pumps/valves and offers advantages such as individual sample addressing, reagent isolation, and compatibility with existing array-based techniques[3-5]. Consequently, digital microfluidics is a promising candidate for many lab-on-a-chip applications. Several biological and chemical functions have been demonstrated using digital microfluidics including glucose assays[6], DNA amplification with polymerase chain reaction[7], purification of peptides and proteins from heterogeneous mixtures[8], and chemical synthesis[9].

Digital microfluidics is generally realized by sandwiching a liquid droplet between two layers of electrodes. One layer has a grounding electrode over its entire surface while the other contains an array of lithographically defined, individually addressable electrodes. A dielectric layer is deposited over the electrodes to provide electrical insulation and prevent electrolysis. Finally, a hydrophobic material coats both the top and bottom layers, which form the fluidic manipulation chamber[1,2]. The design of the aforementioned electrodes is such that a droplet needs to cover one or more electrodes at a time. When a voltage is applied to the electrode at one side of a droplet, the droplet experiences a net electromechanical force that is proportional to the capacitative energy per unit area stored in the dielectric layer[10,11]:

$$F_{net} \sim \frac{\varepsilon_{di}}{d_{di}} V_{di}^2 \qquad (1)$$

where F_{net}, ε_{di}, d_{di}, V_{di} are the net force per unit length, electrical permittivity of dielectric layer material, dielectric layer thickness, and voltage across the dielectric layer, respectively. This electromechanical force results in droplet transport towards the electrode with voltage applied.

In an EWOD system, a large manipulation area requires a large number of lithographically defined electrodes. Given that an EWOD device with a NxN array of electrodes generally requires individual addressing of N^2 electrodes, a large array may require on-chip addressers and decoders, increasing the cost and complexity of the chip substantially. Time-division multiplexing has been proposed to reduce the number of interconnects from N^2 to 2N; however, this places limitations on possible droplet manipulation patterns and reduces overall actuation force[12,13].

Previously, we reported an optoelectowetting (OEW) device[14,15] which removes the need for individual electrode addressing. Instead of electrically addressed interconnects, photosensitive interconnects were used to selectively address electrodes using light. While this device removed the constraint of complex addressing schemes, the size of the manipulated droplet was still governed by the size of the patterned electrodes. We subsequently reported a continuous-optoelectrowetting (COEW) device[16,17] which utilized a continuous photosensitive film replacing both the electrodes and interconnect lines to achieve droplet manipulation. Due to the fact that a thick (0.4 μm) PECVD oxide layer was required to insure a pinhole free oxide, the reported COEW device used a much thicker photoconductor film (5 μm). In addition to a longer

deposition time, film stress must be carefully controlled in this situation because a thick film is prone to cracking and/or delamination. Furthermore, a higher optical power density (e.g. laser) is necessitated in order to fully activate the virtual electrode and enact droplet movement.

In this paper, we report on a new light-actuated digital microfluidics (LADM) device (Fig. 1a). The new device features significant improvements over our previously demonstrated OEW and COEW devices. The LADM device features a thin Al_2O_3 dielectric layer, deposited by atomic layer deposition (ALD), to achieve low-power (both electrical and optical) operation, high reliability, and large actuation area (> 1 cm x 1 cm) with no lithography steps (Fig. 1b). This allows the use of a simple data projector (instead of a laser) to easily perform real-time control of a large number of droplets. This, in turn, enables the demonstration of critical digital microfluidics functionalities such as droplet transport, creation, splitting and merging. Furthermore, the LADM device holds the advantage of easily achieving droplet functionalities such as parallel manipulation and array formation, which are crucial for high-throughput assay-based analyses.

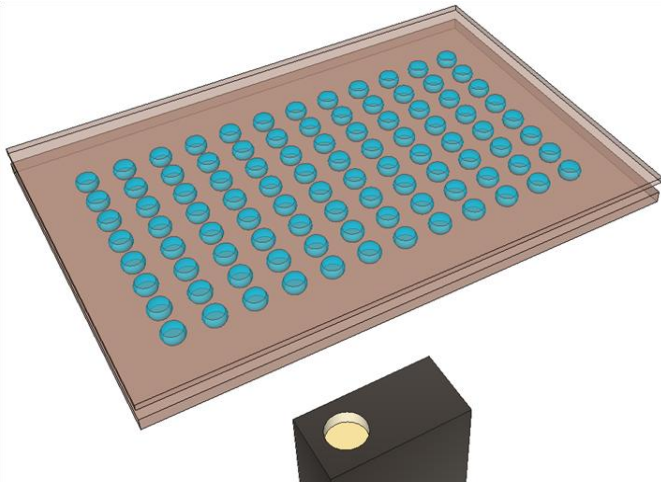

Fig. 1a An artistic impression of the device – droplets on chip are manipulated by a light source

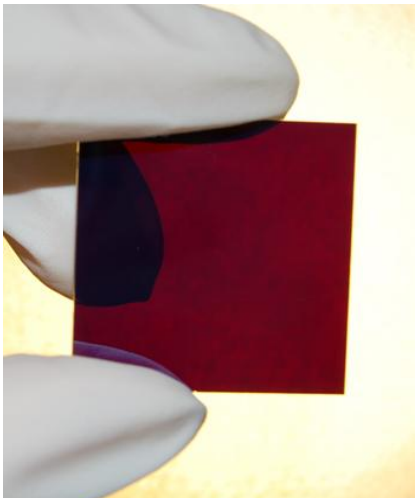

Fig. 1b A fabricated chip, no photolithography step is involved.

Device design, fabrication and operation

1) Design

Fig. 2 illustrates the operating principle of the LADM device. It consists of a microfluidic chamber sandwiched between a photosensitive a-Si:H electrode coated with an electrically insulating oxide layer (bottom) and a transparent electrode (top). In the absence of light, the applied voltage drops primarily across the highly resistive a-Si:H layer. However, upon illumination, the conductivity of the a-Si:H increases by more than 100x[18]. This causes the voltage to drop primarily across the electrically insulating layer. Thus, the illuminated area is analogous to an electrically biased electrode. In other words, it acts as a 'virtual electrode'. If the virtual electrode is created only on a fraction of the droplet's contact line, a net electromechanical force, and subsequent droplet translation, towards the illuminated region will occur.

Low actuation voltage is desired for practical digital microfluidic devices. As is evident from Eq. 1, reducing the dielectric thickness can effectively lower the voltage requirement while maintaining the same actuation force. High dielectric constant materials can also increase the net force on the droplet[19]. The LADM device employs Al_2O_3, whose dielectric constant (~10) is 2.5x higher than SiO_2. Advances in atomic layer deposition (ALD) have made it possible to deposit high quality, conformal, pinhole-free layers of dielectric films on digital microfluidic devices[20]. The film quality is superior to those deposited by plasma-enhanced chemical vapor deposition (PECVD). ALD is also widely used by the semiconductor industry for high-K (high dielectric constant) dielectric deposition in state-of-the-art complementary metal-oxide-semiconductor (CMOS) transistors. Furthermore, by scaling down the dielectric thickness, a corresponding decrease in photoconductive layer thickness to 1 μm can be facilitated, ameliorating much of the film-stress-related issues.

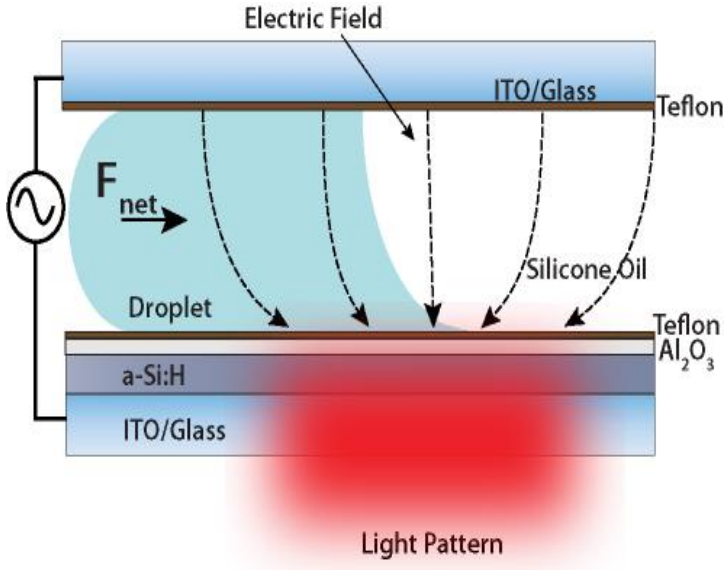

Fig. 2 Device schematic showing incident light creating localized area of high conductivity in the a-Si:H film. This switches the voltage drop from the a-Si:H layer to the oxide layer, and creates localized electric field concentration in the illuminated region. A net electro-mechanical force then acts on the droplet, translating it towards the light pattern.

By modeling the different layers of the LADM device using a lumped-circuit model (Fig. 3a), the force imparted on a droplet as a function of applied frequency and photoconductive layer thickness is simulated using equation 1. A comparison of the resultant relative force per unit contact line length (normalized to the direction of motion) by the legacy COEW device[17] (5 μm a-Si:H photoconductive layer, 0.4 μm SiO_2) and the new LADM device reported here (1 μm a-Si:H photoconductive layer, 100 nm Al_2O_3), plotted against a function of a-Si:H photoconductive layer thickness, is shown in Fig. 3b, using each device's respective oxide material and thickness, at a constant frequency of 10 kHz.. The observation from the relative force calculation is that as the oxide layer is scaled down, a lower frequency and thinner photoconductive layer can be used to achieve the maximum possible actuation force.

Furthermore, as a result of scaling down the photoconductive layer thickness, the amount of optical power necessary for virtual electrode actuation is reduced such that a commercially available data projector can be used to easily generate light patterns for droplet manipulation. The optical pattern of interest is created, in real-time, on a computer and sent to the data projector. The generated light patterns and their movement are easily programmable.

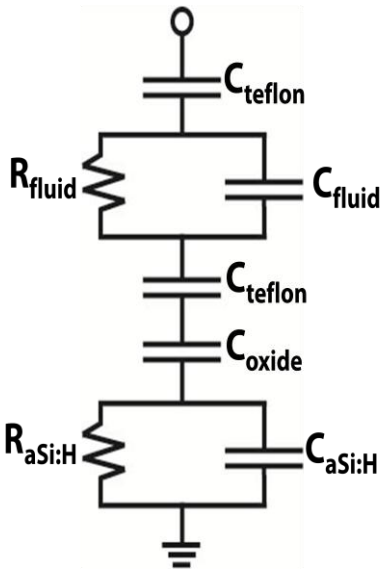

Fig. 3a Equivalent circuit model for different layers in the device

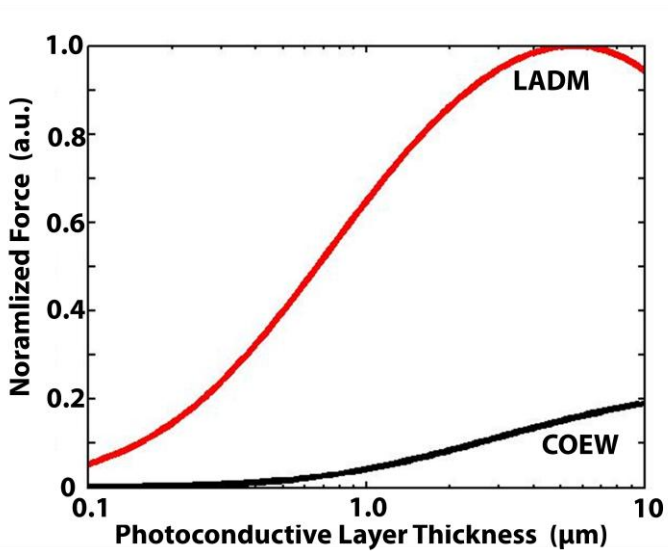

Fig. 3b Normalized force per unit length imparted on droplets as a function of a-Si:H photoconductive layer thickness. At a constant frequency of 10 kHz, LADM aluminum oxide dielectric layer thickness of 100 nm and COEW silicon oxide thickness of 0.4 μm is used.

However, although ALD allows for the aggressive scaling of the dielectric layer, there is a fundamental limit to how thin the layer can be because of dielectric breakdown[19]. As can be seen from Fig. 4, at very thin dielectric thickness, dielectric breakdown (and hence electrolysis) will happen before a droplet start moving. However, at thicker dielectric thickness a droplet will be able to overcome frictional forces on the droplet[22] and move reliably before dielectric breakdown occurs. From Fig. 4, a "good" dielectric thickness around 100 nm can be observed.

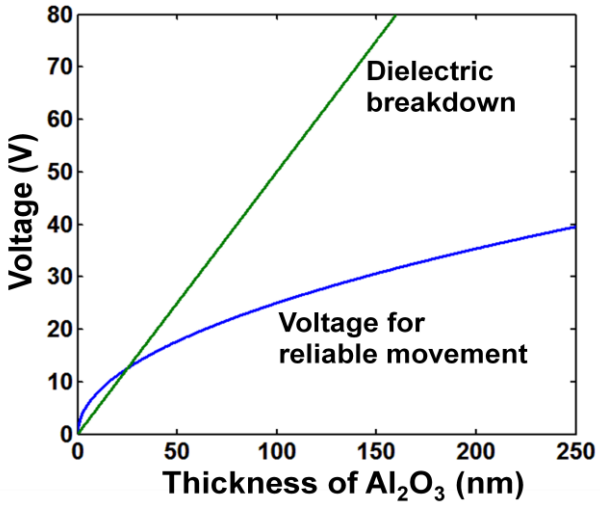

Fig. 4 Thinner dielectric results in less voltage requirement for droplet actuation. However, dielectric breakdown occurs when dielectric layer is too thin. An optimal thickness is around 100 nm.

2) Fabrication

As shown in Fig. 2, the LADM device consists of an indium-tin-oxide (ITO) (300 nm) coated glass substrate, a 1 μm thick photosensitive a-Si:H layer deposited via PECVD (Oxford Plasmalab 80plus), a 100 nm film of Al_2O_3 deposited by ALD (Picosun Sunale R150) and a 25 nm film of spin coated 0.2% Teflon (3000 rpm, 30 s). The top electrode is made of another Teflon-coated ITO glass wafer. It is worth noting that the fabrication process does not require any photolithography. Potentially, the LADM devices can be mass produced at very low cost. The two substrates are then placed on top of one another separated by a spacer layer of double-sided tape (100-500 μm) forming a microfluidic chamber. The total manipulation area on-chip is currently 1.6 cm x 1 cm. A physical image of the device is shown in Fig. 1b.

3) Operation

Fig. 5 shows the droplet manipulation setup. AC bias is applied to the top and bottom ITO substrates. A commercially available projector (Dell 4210X DLP) is projected onto the device substrate which provides ~1 W/cm^2 of optical power (versus 254 W/cm^2 laser for the COEW device[17]. Optical patterns are generated on an external computer and sent to the projector. Bright-field illumination, a continuous zoom microscope (Navitar 12X), and a CCD camera (Sony XCD-X710) are used for visualization and recording. No external optical lenses other than those intrinsic to the projector and microscope are required, making the set-up easy to assemble, use and transport. During operation, the fluidic chamber is first flooded with silicone oil (1.0 cSt DMS Trimethylsiloxy-terminated Polydimethylsiloxane, Gelest Inc. Morrisville, PA) to reduce evaporation and friction. Aqueous droplets or reservoirs (10 mS/m deionized water with added KCl) are then introduced into the fluidic chamber via a syringe pump (KD Scientific, 780210) and Teflon tube (Cole-Parmer Microbore PTFE). A remark here is that all polar liquids can be manipulated in the device as long as the liquid impedance is considerably less than that of the oxide and a-Si:H. Liquids including acetone, PCR buffers, and de-ionized water have all been observed to manipulate well using the device.

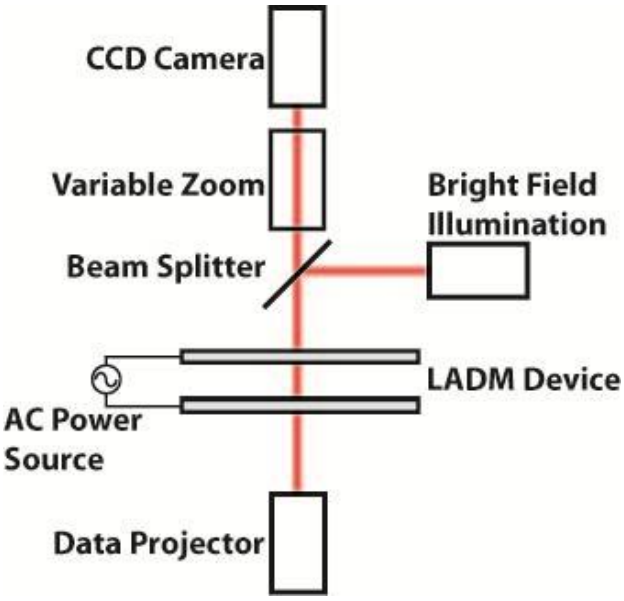

Fig. 5 Experimental setup. A standard data projector (spatial light modulator) is focused onto the light-actuated digital microfluidics substrate, a CCD camera allows for droplet visualization.

Experimental results and discussion

Using atomic layer deposition, we are able to scale down the LADM's oxide and photoconductive layers. This, in turn, reduces the voltage and optical requirements necessary to actuate droplets. In this section, we first demonstrate critical digital microfluidics functionalities of droplet transport, separation, merging, and creation from a reservoir. We then demonstrate functionalities not easily achieved using EWOD based digital microfluidics, namely manipulation of different sized droplets, multi-droplet manipulation and droplet array formation.

1) Droplet transport

To investigate droplet transport speed dependence on applied voltage, square light patterns were projected onto droplets with varying diameters and thicknesses (the droplet volumes are 190 nL and 85 nL for 300 μm thickness, and 64 nL and 28 nL for 100 μm thickness, respectively, determined by the gap spacing between the top and bottom substrates). The resulting maximum droplet actuation speeds were recorded for various applied voltages (Fig. 6a and Fig. 6b) at a frequency of 10 kHz. A maximum speed of 2 cm/s was achieved at 52 Vppk. Compared with prior work on COEW, the current device has 20x faster manipulation speed while using 5x lower voltage and 250x lower optical intensity. Droplets can be actuated with lower voltage bias, though at reduced speed (as per the quadratic dependence of actuation force on voltage (Eq. 1)). Droplet translation with speed ~0.5 mm/s at voltages as low as 16 Vppk is achieved and the voltage applied is amongst the lowest reported for digital microfluidics. At high voltages, the actuation speed deviates from the quadratic relationship with respect to voltage as predicted by Eq. 1 due to larger frictional forces acting on the droplet when speed increases[21,22].

Similarly, to investigate droplet transport speed dependence on applied frequency, square light patterns with sizes similar to the diameter of the manipulated droplet were projected onto droplets of different heights and diameters. The resulting maximum speeds of droplet actuation were recorded for various applied frequencies (Fig. 7a and Fig. 7b) at an applied voltage of 40 Vppk. A droplet actuation window of 1 kHz to 10 kHz was observed. As a side note, this frequency window can be controlled by varying the thickness of layers in the device stack. The noticeable speed increase between 100 kHz to 1 MHz in Fig. 7b has been attributed to dielectrophoretic forces acting on the droplet (instead of electrowetting force at lower frequency). We have made use of this dielectrophoretic force regime to realize both LADM and optoelectronic tweezer[23] functionalities on the same chip, enabling applications such as particle concentration and single cell encapsulation[24].

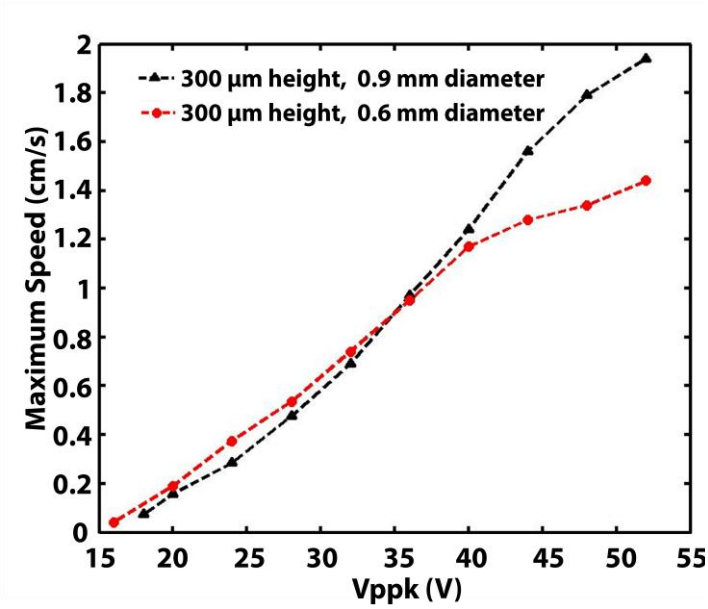

Fig. 6a Maximum droplet speed versus voltage for two droplets at 300µm height and different diameters (10 kHz frequency).

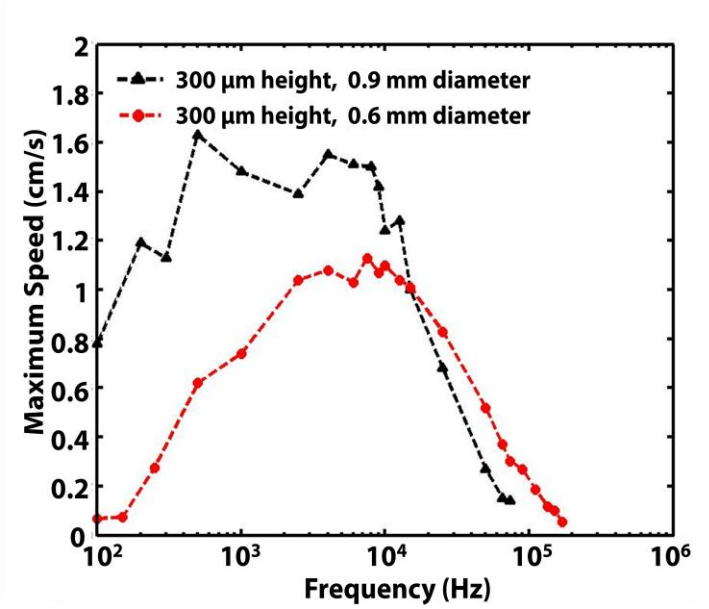

Fig. 7a Maximum droplet speed versus frequency for two droplets at 300µm height and different diameters (40 Vppk).

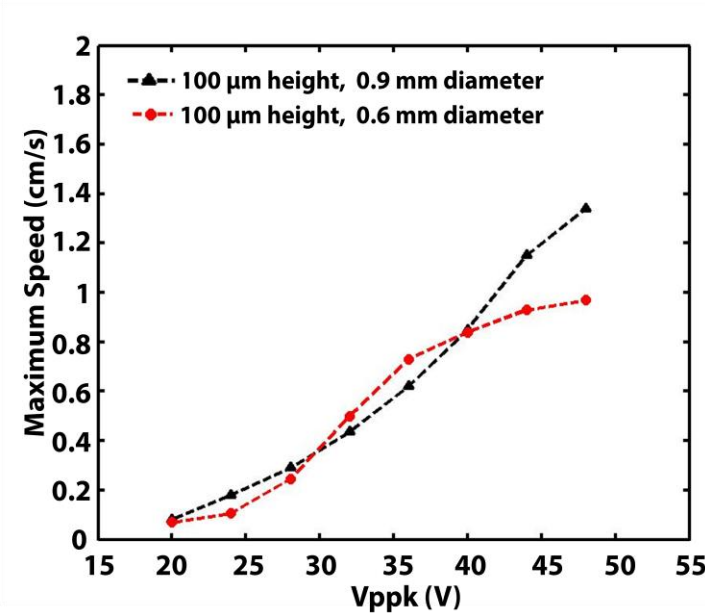

Fig. 6b Maximum droplet speed versus voltage for two droplets at 100µm height and different diameters (10 kHz frequency).

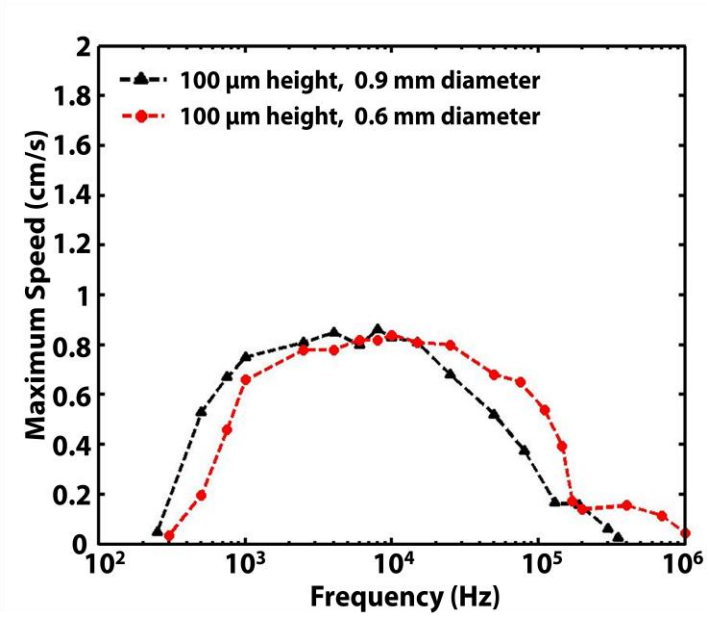

Fig. 7b Maximum droplet speed versus frequency for two droplets at 100µm height and different diameters (40 Vppk).

2) Droplet separation and merging

The ability to separate and merge droplets is a critical component of any digital microfluidic system because chemical reactions require reagents to be added or separately analyzed. In Fig. 8a, two light patterns (1.15 mm x 1.30 mm) move two individual 900 nL droplets towards each other until they merge into one large droplet (1800 nL). Fig. 8b demonstrates the splitting of an 1800 nL droplet into two 900 nL droplets. This is achieved by moving two light patterns in opposite directions.

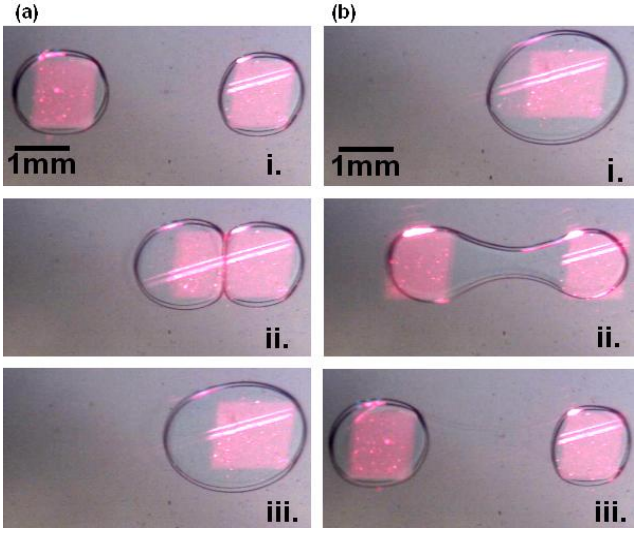

Fig. 8a Droplet Merging. Two 900 nL droplets (i) are merged (ii) by moving one light pattern towards the other resulting in a single droplet (iii) (50 Vppk, 10 kHz).

Fig. 8b Droplet splitting. A single 1800 nL droplet (i) is pulled apart using two light patterns, with one pattern moving towards the left (ii), resulting in two distinct droplets (iii) (50 Vppk, 10 kHz).

3) Droplet creation from reservoir

The ability to create droplets from on-chip reservoirs is important for realizing true lab-on-a-chip functionalities (e.g. removing the need for off-chip pumps and lines). In Fig 9, we demonstrate the creation of a droplet from a reservoir. The reservoir can be defined anywhere on the chip by using a larger light pattern to pin down the reservoir, a smaller light pattern then extracts droplets out of the reservoir. In this demonstration, a smaller light pattern (~1mm x 1mm) extracts droplets out of the reservoir sequentially. A total of 96 droplets were pulled out of the reservoir at a speed of 5.5 seconds per droplet. The average volume per droplet is 120.44 nL with a standard deviation of 2.67 nL.

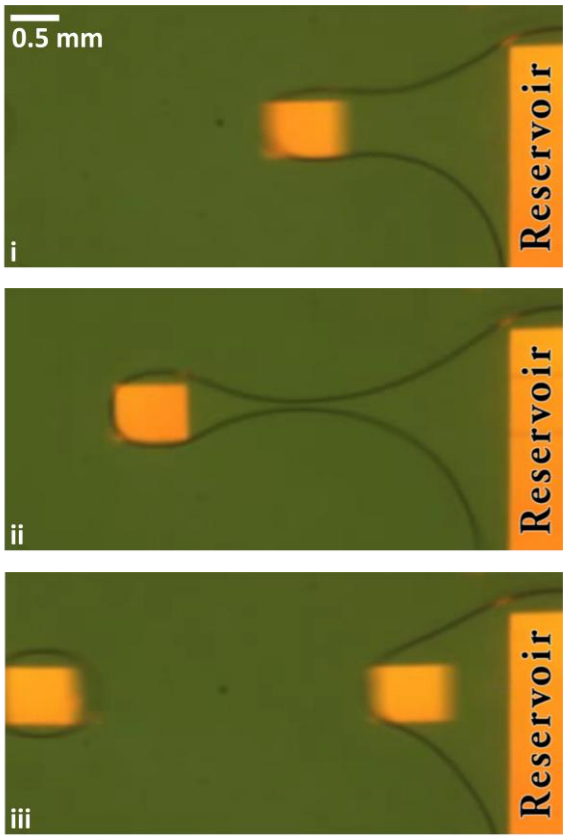

Fig. 9 Dispensing a 120 nL droplet from a reservoir. A bigger light pattern pins down the reservoir while a smaller light patterns pulls out a droplet from the reservoir, each droplet is generated in 5.5 seconds. A total of 96 droplets are generated from this reservoir sequentially (60 Vppk, 10kHz).

4) Different sized droplet manipulation

Manipulation of different sized droplets is not easily achieved using conventional digital microfluidics devices due to the fixed electrode size. LADM addresses this issue easily by simply changing the size, shape and number of the optical patterns to define different virtual electrodes. Droplets with a wide range of volumes can be manipulated on the same chip which enables applications where droplet size changes over the course of the application (e.g. addition of reagents during chemical/biological processing). In the demonstration of Fig 10, two droplets of 3.3 μL and 190 nL (17x volume difference) are manipulated simultaneously on the same chip device surface. Since the chamber height is fixed, the maximum limit of this droplet volume ratio, given the current manipulation area, is around 100x.

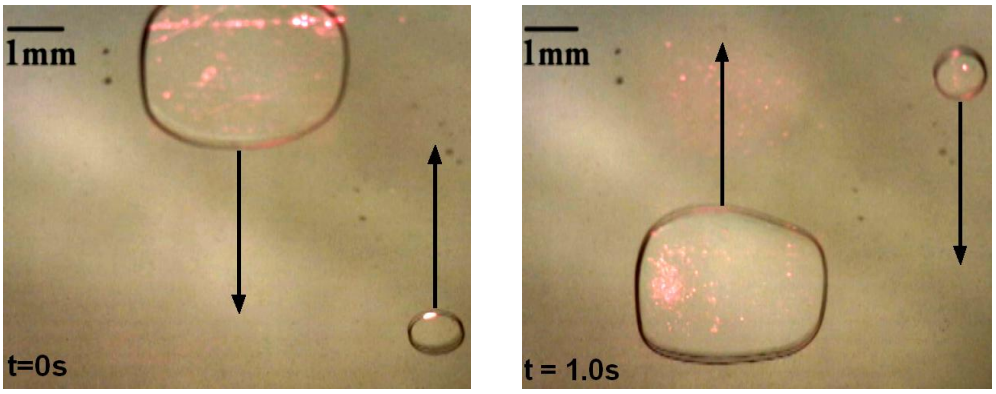

Fig. 10 Manipulation of bigger (3.3 μL) and smaller (190 nL) droplets on the same device surface, the volume differs by ~17 times (40 Vppk, 10kHz).

5) Multi-droplet parallel manipulation and array formation

The ability to manipulate multiple droplets in parallel and form droplet arrays is important for many high throughput assay applications. This is a task well suited by LADM as parallel manipulation is achieved simply by altering the projected optical patterns. Fig. 11a demonstrates LADM's ability to effect real-time, reconfigurable droplet manipulation. The simultaneous movement of 7 droplets is demonstrated. The 4 outer droplets move clockwise in a circular manner, whilst the 3 inner droplets move anti-clockwise. Fig. 11b shows a 96-droplet (8 by 12) array formed using the LADM device. Light patterns extract 220 nL droplets dispensed from a Teflon tube and arrange the droplets into a horizontal column of 12 droplets before transporting them into an array. These demonstrations show that the LADM device is well suited to directly miniaturize and automate assay-based biological or chemical analysis currently performed using well-plates and pipettes. This allows large numbers of reactions to occur in parallel using small reagent volumes, decreasing analysis turn-around time and reagent cost. In addition, the automation of optical pattern generation and feedback will greatly decrease the number of manpower hours required to perform time-consuming assay tasks.

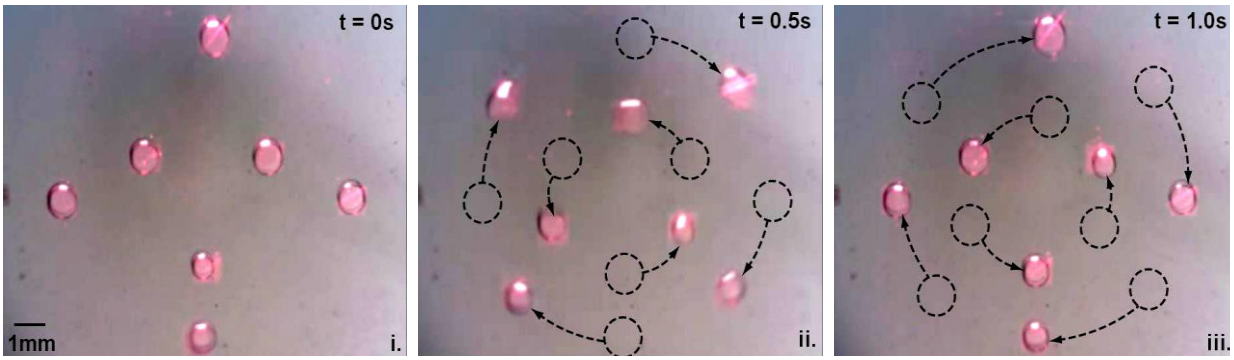

Fig. 11a Parallel movement of droplets. 7 droplets undergo simultaneous movement. 4 outer droplets moves clockwise in a circular manner, whilst 3 inner droplets move anti-clockwise in a circular manner (200 nL, 50 Vppk, 10 kHz).

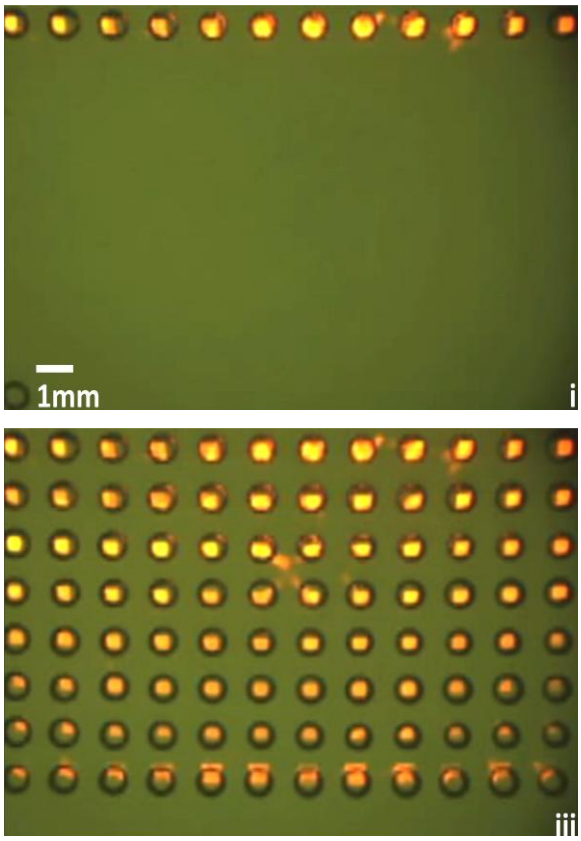

Fig. 11b On-demand formation of a parallel array of droplets. Projected light patterns pull twelve 220 nL droplets dispensed from a Teflon tube and arrange the droplets into a horizontal column before transporting the droplets into a 8x12 array (60 Vppk, 10 kHz).

Conclusion

We have presented a light-actuated digital microfluidics device that is capable of creating arbitrarily-sized electrodes without complex addressing schemes. This technique provides many advantages over current droplet manipulation methods including ease of fabrication, a simple manipulation set-up for light generation and imaging, and the ability for real-time, parallel, reconfigurable droplet control. The use of an ALD oxide layer allows one to aggressively scale oxide thickness which subsequently reduces the required voltage and optical power necessary to achieve high speed actuation (2 cm/s). By reducing the optical power demands, a simple data projector can be used to pattern the virtual electrodes over a large area on the LADM surface. Using this technique, we have successfully demonstrated many of the critical operations (e.g. creation, splitting, merging, and transportation) required of digital microfluidics as well as shown the ease to which this technique allows for the parallel manipulation of arbitrarily-sized droplets. The light-actuated digital microfluidics device is a promising candidate to realize a powerful, easy to use platform for large-scale lab-on-a-chip analyses.

Acknowledgement

The authors would like to thank the UC Berkeley Marvell Nanolab where all devices were fabricated. This work was supported in part by the Berkeley Sensor and Actuator Center (BSAC) and the Center for Cell Control, a NIH Nanomedicine Development Center, under grant PN2 EY018228.

Reference

1. M. G. Pollack, R. B. Fair, and A. D. Shenderov, *Appl. Phys. Lett.*, 2000, **77**, 1725-1726.
2. S. K. Fan, H. Moon, and C. J. Kim, *J. Microelectromech. Syst.*, 2003, **12**, 70-80.
3. R. B. Fair, *Microfluid. Nanofluid.*, 2007, **3**, 245-281.
4. M. Abdelgawad and A. R. Wheeler, *Adv. Mater.*, 2009, **21**, 920-925.
5. S. Teh, R. Lin, L. Hung, and A. P. Lee, *Lab Chip*, 2008, **8**, 198-220.
6. V. Srinivasan, V. K. Pamula, and R. B. Fair, *Analytica Chimica Acta*, 2004, **507**, 145-150.
7. Z. Hua, J. L. Rouse, A. E. Eckhardt, V. Srinivasan, V. K. Pamula, W. A. Schell, J. L. Benton, T. G. Mitchell, and M. G. Pollack, *Anal. Chem.*, 2010, **82** (6), 2310-2316.
8. A. R. Wheeler, H. Moon, C. A. Bird, R. R. Loo, C. J. Kim, J. A. Loo, and R. L. Garrell, *Anal. Chem*, 2005, **77**, 534-540.
9. J. R. Millman, K. H. Bhatt, B. G. Prevo, and O. D. Velev, *Nat. Mater.*, 2005, **4**, 98-102.
10. T. B. Jones, J. D. Fowler, Y. S. Chang, and C. J. Kim, *Langmuir*, 2003, **19**, 7646-7651.
11. F. Mugele and J. Baret, *Journal of Physics: Condens. Matter*, 2005, **17**, R705-R774.
12. J. Gong and C. J. Kim, *Micro Electro Mechanical Systems (MEMS), IEEE 18th International Conference*, 2005, **18**, 726-729.
13. J. Gong, S. K. Fan, and C. J. Kim, *Micro Electro Mechanical Systems (MEMS), IEEE 17th International Conference*, 2004, **17**, 355-358.
14. P. Y. Chiou, H. Moon, H. Toshiyoshi, C. J. Kim, M. C. Wu, *Sens. Actuat. A: Phys*. 2003, **104** (3), 222-228.
15. P. Y. Chiou, Z. Chang, and M. C. Wu, *J. Microelectromech. Syst.*, 2008, **17**, 133-138.
16. P. Y. Chiou, Z. Chang, and M. C. Wu, *Tranducers, Solid-State Sensors, Actuators and Microsystems, IEEE 12th International Conference*, 2003, 1, 468-471.
17. P. Y. Chiou, S.- Y. Park, and M. C. Wu, *Appl. Phys. Lett.*, 2008, **93**, 221110-221113.
18. J. K. Valley, A. Jamshidi, A. T. Ohta, H.- Y. Hsu, M. C. Wu, *J. Microelectromech. Syst.*, 2008, **17**, 342-350
19. H. Moon, S. K. Cho, R. L. Garrell, and C. J. Kim, *J. Appl. Phys.*, 2002, **92**, 4080-4087.
20. B. Raj, M. Dhindsa, N. R. Smith, R. Laughlin, J. Heikenfeld, *Langmuir* 2009, **25** (20), 12387-12392
21. M. G. Pollack, A. D. Shenderov, and R. B. Fair, *Lab Chip*, 2002, **2**, 96–101.

22. V. Bahadur and S. V. Garimella, *J. Micromech. Microeng.*, 2006, **16**, 1494-1503.

23. P. Y. Chiou, A. T. Ohta and M. C. Wu, *Nature*, 2005, **436**, 370–372.

24. J. K. Valley, S. N. Pei, A. Jamshidi, H.- Y. Hsu, and M. C. Wu, *Lab Chip*, 2011, 10.1039/c0lc00568